Finite Element Modelling of Geogrids Reinforced Ballasted Tracks

Trung Ngo, PhD, CPEng, MASCE

Senior lecturer, School of Civil and Environmental Engineering, Faculty of Engineering and Information Technology, University of Technology Sydney, Ultimo, Australia. Email: Trung.Ngo@uts.edu.au

Maheer Hasan

Geotechnical Engineer, WSP, Australia Email: maheerhasan@outlook.com

Technical Paper, Submitted to: **Transportation Infrastructure Geotechnology**

Author for correspondence:

Dr Trung Ngo

School of Civil and Environmental Engineering

Faculty of Engineering and Information Technology

University of Technology Sydney

15 Broadway, Ultimo, NSW 2007

Australia.

Phone: +61 2 9514 5989

Email: Trung.Ngo@uts.edu.au

Declarations

- **Ethics approval and consent to participate**

  Not applicable

- **Consent for publication**

  Not applicable

- **Availability of data and materials**

  The datasets used and/or analysed during the current study are available from the corresponding author on reasonable request.

- **Competing interests**

  The authors declare that they have no competing interests

- **Funding**

  Not applicable

- **Authors' contributions**

  Trung Ngo: Supervision, Conceptualization, Analysis, investigation, Writing, reviewing & editing. **Maheer Hasan**: Numerical modelling, Analysis, Writing, reviewing & editing.

- **Acknowledgments**

This research work has been carried out during the Capstone project at the School of Civil and Environmental Engineering (CEE), Faculty of Engineering and Information Technology, University of Technology Sydney. The authors acknowledge the support and assistance from UTS-IT officers for assistance in using the iHPC and WorkSpace for FEM simulations during this Capstone project.

- **Declare your total self-citations**

I confirm that the total self-citation is only 2 in this manuscript.

Finite Element Modelling of Geogrids Reinforced Ballasted Tracks

ABSTRACT:

This paper presents results obtained from three-dimension Finite Element Modelling (FEM) to study the effects of geogrids on the deformation responses of ballasted tracks. In this study, a series of numerical simulations are carried out on track sections with and without the inclusion of geogrids. Sensitivity analysis was carried on parameters affecting the performance of geogrid, including the axial stiffness, interface property, and the location of geogrid placement in the track substructure. The tracks are subjected to moving train loading under 150 kN wheel load travelling at a given speed of 72km/h. Based on simulation results, it is found that geogrid provides a reinforcing function to rail track primarily in the form of confinement which resulted in reduced lateral displacement in a reinforced track compared to a traditional track. A significant reduction in vertical and lateral displacement is found from the inclusion of a geogrid layer at the ballast and capping interface while the effect of geogrid reinforcement is more pronounced with increased loading cycles. The effects of geogrid stiffness, interface conditions and geogrid placement are studied and it is found that the axial stiffness of geogrid is found to impact overall track deformation while the optimum placement of geogrid is found to directly at the ballast and capping interface.

Keywords: Ballast, Geogrid, Track deformation, Interface property, Finite Element Modelling

1. Introduction

Railway forms the largest network of public and freight transportation, due to its capability to deliver heavy carrying capacities at relatively fast speeds (Selig and Waters, 1994). Rail tracks are often built on ballasted beds that provide structural support and resiliency to cyclic loads, produced by railway vehicles (Esveld, 2014; Powrie et al., 2019). However, these ballasted rail tracks are prone to periodic maintenance requirements due to the breakage and fouling of ballast, which cause deformation of the track (Le Pen et al., 2018; Tutumluer et al., 2013). The recurrent maintenance requirements usually necessitate significant rehabilitation cost, operation delays and lower travel speeds (Giannakos, 2010). Ballasted tracks have been implemented abundantly throughout Australia's rural and urban transport networks, are known to be prone to this problem of recurrent degradation and maintenance. There are some advantages that can be attained through ballasted track, in comparison other systems, such as the slab tracks. This includes lower initial capital cost, typically easier rail track construction and alignment process, and relatively good drainage (Setiawan, 2016).

Whilst ballasted tracks offer advantages, it is clear that the current design and configuration of present significant challenges to lifecycle operation and maintenance. This is primarily due to the susceptibility of ballast to experience progressive degradation due to cyclic loading, which allow track fouling, differential deformation, and pumping of subgrade soils (Indraratna et al., 2023; Nazari et al., 2022). From an environmental view, rail network is seen to provide advantages over road transport; however, the implementation of faster travel times and frequent services will be required to make rail an attractive option for commuter use. Yet, with faster and heavier freight trains, there is concern of greater noise, vibration and other pollution sources, and hence, it is necessary for industry to continue to analyse, study and mitigate adverse effects of these issues.

Geogrid are comprised of synthetic material such as polyester and functions primarily to provide reinforcement (Brown et al., 2007a; Brown et al., 2007b; Luo et al., 2023b; Ngo et al., 2016). A planar geogrid like material that consist of parallel sets of tensile ribs with openings known as apertures that lock granular or soil material in place (Duncan-Williams and Attoh-Okine, 2008; Li et al., 2015). Geogrid in particular has been proven to be effective in rail track application reducing potential of track displacements. Having placed in ballasted tracks, geogrids provide confinement and prevents the lateral movement of ballast, which correspondingly reduces track deformation and vertical settlement (Chen et al., 2013; Chua et al., 2023; Feng and Wang, 2023; Hussaini et al., 2016). Previous studies have indicated that

the inclusion of a geosynthetics layer is an effective method to mitigate the breakage, fouling and degradation of ballast (Tutumluer et al., 2012).

One of the major issues in rail track engineering is the problem of differential settlements, which typically is caused due to the lateral spread and degradation of ballast. This deformation of the ballast layer causes misalignment of the track geometry, requiring frequent maintenance work (Shan et al., 2020). Therefore, the role of geogrids in railway track is to reduce the lateral displacement of ballasted material and provide confinement. Reinforcement is dependent on a level of interlock between a geogrid and aggregates (Fisher and Horvat, 2011). From this interlock, a reduction in irrecoverable strains above the zone of influence of the grid will occur, which in turn reduces vertical deformation of ballast (Luo et al., 2023a).

There are several factors that affect the performance of geogrids in rail track such as the aperture shape and size, material stiffness, interface conditions, and placement location of the grid (Bathurst et al., 2009; Brown et al., 2007b). Jiang and Nimbalkar (2019) indicated that subgrade conditions can impact the rate of reinforcement that is offered by geogrid. In this study, a three dimension (3D) Finite Element Modelling (FEM) via software package PLAXIS 3D is used to study the factors affecting the performance of geogrid. In particular, the impact of varying the grid stiffness, interface and placement of the grid is investigated. Geogrid can be placed at several different locations of the track. Many agree that the optimum locations of grid placement are typically either at the interface between ballast and capping (sub-ballast), or near the transition to subgrade (Brown et al., 2006; Indraratna et al., 2023). One or more layers of geogrid may be used, depending on the requirements of the track and expected loading conditions.

Nonetheless, the interface behaviour between geogrid-ballast has not fully been studied or properly considered in track design and the mechanisms of geogrid reinforcement are still subject to further study. This is significant as interface properties govern the ability ballast to displace, and therefore the track to exhibit settlement. Furthermore, limited studies (and technical capacity) is available to model long-term behaviour of rail track. For example, the Discrete Element Method (DEM) is a valuable tool that enables characterisation of the individual granular particle behaviour and particle breakage which is an ability that FEM does not possess (Feng and Wang, 2023; Konietzky et al., 2004). However, DEM necessitates high computational times and therefore, is currently unable to model high number of loading cycles. FEM can provide better ability to simulate long-term behaviour, but is not able to represent complex behaviour of ballast and the consequences this has to ballast-geogrid interlocking

(Dong et al., 2010; Li et al., 2010). Hence, while the efficacy of geogrid reinforcement is understood, it is seen that there are some limitations that barrier the implementation of the solution.

The main objective of paper is to quantify the effects of geogrid reinforcement in ballasted rail track using 3D numerical analyses that are performed to compare the load-deformation responses between a conventional unreinforced and geogrid reinforced ballasted tracks. This will include examining the role of geogrid has on track settlements, lateral displacements that occurred during train loading. In addition, the paper presents a parametric study on the effect of varying geogrid parameters including the grid stiffness (EA), interface properties (R_{inter}) and location of geogrid reinforcement. Ultimately, the intent is to contribute to the current understanding of ballasted track design with the adoption of geogrid reinforcement and FEM modelling of geogrid reinforced track.

2. Numerical Analysis of Rail Tracks

Modelling of rail track substructures have been carried out using either analytical or numerical models. Li et al. (2015) reported four methods that are commonly used to analyse the behaviour of rail track and subgrade, which are namely the: (i) elastic half space model, (ii) beam elastic foundation (BOEF) model, (iii) multilayer models, and (iv) finite element models (FEM). However, the elastic half space and BOEF models are often required some assumptions for the development of track and subgrade models due to oversimplification of foundation conditions, complexities related to the use of equations and charts. Current accessibility to multi-layered computational models such as FEM which can characterise actual geotechnical conditions with much more accuracy (Moghadam and Ashtari, 2020; Sayeed and Shahin, 2023). Finite element method (FEM) is of interest to this study as it has demonstrated success in the analysis of geotechnical problems, including rail track analysis, pavement design and soil-structure interaction (Alabbasi and Hussein, 2021; Basudhar et al., 2008; Perkins and Edens, 2002; Varandas et al., 2020), among others.

2.1 Finite Element Modelling for Ballasted Tracks

Finite element modelling rail tracks often involve modelling a segment of track and may only include half of the track cross section if the geometry is symmetric along its longitudinal axis. The type and size of the FEM element mesh can be varied (e.g., rectangular, triangular, brick

elements) depending on the degree of accuracy and computational time required. Two-dimensional (2D) or 3D model geometries may be developed for substructure analysis, with each providing certain advantages and disadvantages (Hadi and Alzabeebee, 2023). Analysis of tracks in a 2D problem either in the longitudinal direction or perpendicular to sleepers can be utilised adopting the plane strain condition. Li et al (2015) indicated that a 2D representation may not be an accurate characterisation of the track, due to the inability of the model to include discrete wheel loads and sleeper support along the length of the track. The current FEM analysis is inspired by the research done by Indraratna et al. (2023) in their 2D analysis on the influence of geogrid reinforcement in ballasted railway track. The geometry of track is therefore modified and extended from the aforementioned work to suit 3D conditions.

2.2 **Model Geometry**

A ballasted track employed in this study consists of steel rails, concrete sleepers, ballast (quarried aggregates), capping layer (sub-ballast), and subgrade (natural foundation). Initially, the model was calibrated to fit the recommendations set by previous studies, including Faizan et al (2022), with a 40 x 20 x 10 m (x, y, z axes) geometry adopted. This dimension was considered to allow better representation of impact force and shear wave effects on foundational soils. However, due to limited computational power, this approach was deemed inappropriate. The model therefore adopted, considers a model size of 20 m, 12 m, and 3 m in three directions which sustains the ability to define loading conditions and analyse effects of substructure deformation, as illustrated in Figure 1. Rails were assumed to be continuous welded rail (CWR), spanning the whole length of the track without any intermediate joints, and are simulated using 'Beam' elements. Rails were defined as a solid rectangular beam with a width and height of 50 mm and 160 mm, respectively. This method of approximating the rails is commonly adopted to provide a total area nearly equal to the Australian 60 kg/m rail. Sleepers were modelled with the length, width and height (x, y, z) as 2500 mm, 250 mm and 200 mm, respectively. The sleepers were assumed to be comprised of concrete, with stiffness properties adopted from Jiang and Nimbalkar (2019) and Indraratna et al. (2012), as presented in Table 1. A sleeper spacing of 0.5 m was adopted in the simulation as it is recommended for freight lines, considering the spacing of sleepers at rail joints in plain ballasted tracks. Since the length of the track is 20 m, a total of 41 sleepers were required to be modelled across the track. The superstructure elements in the model include only the sleeper and rail. The inclusion of a fastening system was not considered in the model. The ballast and capping layers are

350mm and 150mm in thickness, respectively, resting over a homogenous subgrade of 3m in thickness.

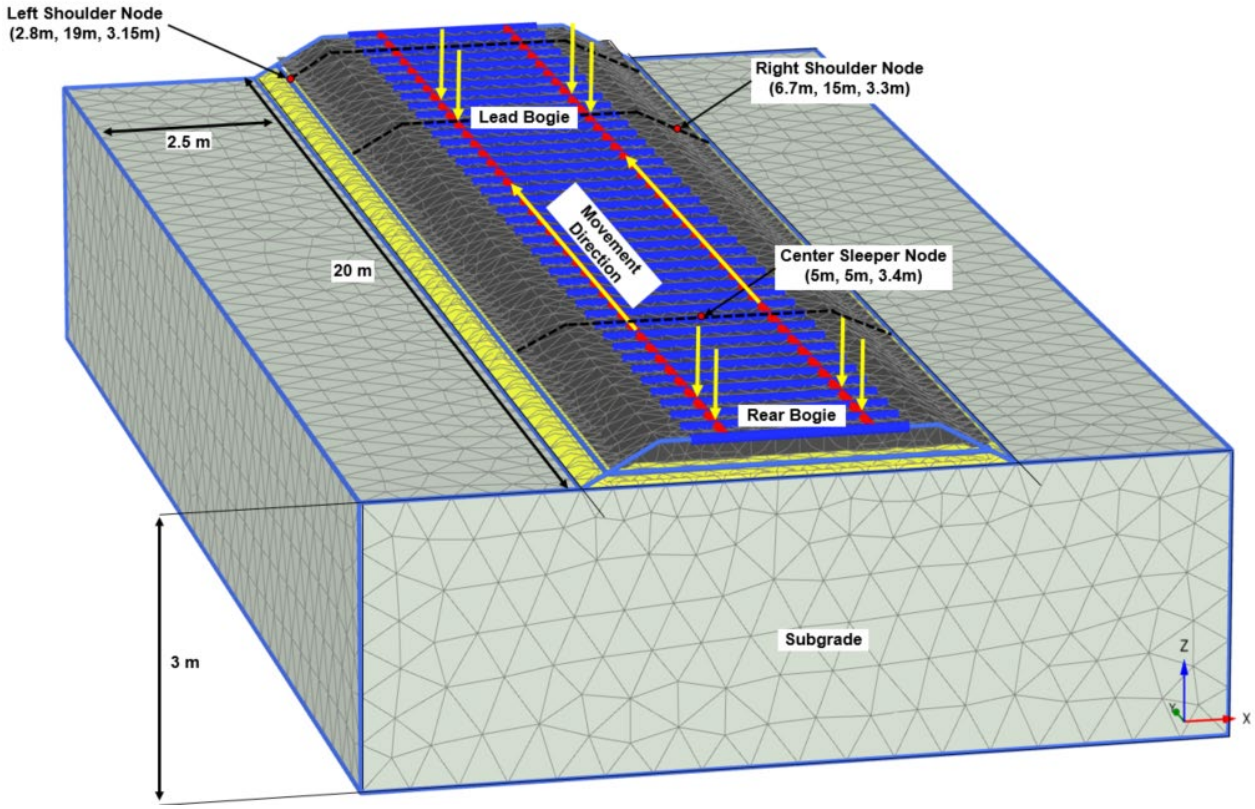

Figure 1. 3D Finite Element Model used for track analysis in this study

2.3 **Material Model and Parameters**

It is noted that the property parameters (e.g., density, Elastic modulus E, Poison's ratio ν, cohesion c, friction angle Φ, and dilatancy angle ψ) of the ballast, capping and subgrade layers influence the simulation results. The above material parameters can be derived from laboratory tests performed on the capping and subgrade materials, such as oedometer tests, large-scale direct shear tests, and triaxial tests, among others. Due to the brevity of this current Capstone project, the material model and parameters used in the current analysis were adopted from the previous studies by Jiang and Nimbalkar (2019), with some parameters (such as void ratio, stiffness, hardening parameters) taken from literature (Gamal et al., 2016; Indraratna et al., 2023; Tucho et al., 2022; Yap et al., 2017; Indraratna et al. 2012). The steel rail and concrete sleeper were modelled as linear-elastic materials since non-yielding behaviour was adopted.

Subgrade soils were assumed to be fined-grained, cohesive soils in a generally stiff condition. Ballast was simulated using the hardening soil (HS) model and the material parameters were selected from Indraratna et al. (2023). Mohr-Coulomb models were used for the capping and subgrade soils to simplify the analysis as well as to achieve reasonable required computational resources. A small value of cohesion (1 kPa) for ballast and capping was utilised to enhance the numerical stability. Friction angles of ballast, capping and subgrade were determined as $\Phi = 58^0$, 35^0 and 20^0 respectively, and these values were determined from direct shear tests while angles of dilation, $\psi = 13^0$ was determined from triaxial tests. A summary of models and parameters adopted in the current FEM analysis are presented in the Table 1.

Table 1. Material properties employed in the current FEM analysis (parameters adopted from Jiang and Nimbalkar 2019 and Indraratna et al. 2012)

Parameter	Ballast	Sub-ballast	Subgrade	Concrete Sleeper	Rail
Soil Model	Hardening Soil	Mohr-Coulomb	Mohr-Coulomb	Linear Elastic	Linear Elastic
Type	Drained	Drained	Drained	Solid	Solid
$\gamma_{unsaturated}$ (kN/m^3)	15.67	16.67	15	-	-
$\gamma_{saturated}$ (kN/m^3)	16	17	17	-	-
γ (kN/m^3)	-	-	-	24	78
E (kN/m^2)	-	80,000	25,000	10,000,000	21,000,000
E_{50}^{ref} (kN/m^2)	21,340	-	-	-	-
E_{oed}^{ref} (kN/m^2)	21,340	-	-	-	-
E_{ur}^{ref} (kN/m^2)	64,020	-	-	-	-
v	-	0.35	0.3	0.15	0.15
v_{ur}	0.2	-	-	-	-
c (kN/m^2)	1	1	10	-	-
Φ (°)	58	35	20	-	-
Ψ (°)	13	0	0	-	-
p_{ref}	50	-	-	-	-
m	0.5	-	-	-	-
k_0^{nc}	0.3	-	-	-	-

R_f	0.9	-	-	-	-
R_{inter}	1	1	1	-	-

E: modulus of elasticity; E_{50}^{ref}: secant stiffness at 50% strength; E_{oed}^{ref} : unloading/reloading stiffness; γ: unit weight; E_{oed}^{ref} : tangent stiffness; ν: Poisson's ratio; v_{ur}: Poisson's ratio for unloading/reloading conditions; c: cohesion; ψ: dilatancy angle; Φ: friction angle; m: stress dependent stiffness factor; p_{ref} : reference confining pressure; k_0^{nc} : coefficient of earth pressure at rest; R_{inter}: interface strength reduction factor; R_f : failure ratio.

2.4 **Model Meshing, Loading and Boundary Conditions**

In the current FEM analysis, 10-node tetrahedral elements are created in the 3D mesh procedure. This element type provides a second-order interpolation of displacements. For tetrahedral elements there are three local coordinates (ξ, η and ζ) and the shape functions N_i have the property that the function value is equal to unity at node i and zero at the other nodes. After conducting mesh sensitivity analysis, a mesh generated in the current FEM model considered as medium coarseness, including 10,095 elements, and 20,112 nodes (Fig. 1).

Moving train loading on the track was simulated as the passage of bogie loads with an initial velocity of 20 m/s (i.e., train speed of 72 km/h) and wheel load of 150 kN, simulating a typical freight train in Australia. Centre-centre axle loads were spaced as 1 meter apart, with bogies spaced 15 meters, which may be considered an approximation of a typical Australian freight trains (Figure 2). Moving loads were generated using the point loads with a movement function to be defined at the aforementioned train speed. A dynamic loading phase was activated to simulating moving train loading with a time interval of 1.0 second. As the train speed was assumed to be 20 m/s with the track being 20 m long; hence, the rear bogie loading was expected to arrive at the boundary by approximately 1.0 second. Prior to calculation, the boundary conditions are defined while the vertical boundaries (right, left and the longitudinal boundaries were assumed as roller supports allowing vertical displacements to simulate relative vertical soil movements.

Rayleigh viscous damping is used in the current 3D-FEM analysis to simulate the damping of track substructure layers and geometric attenuation, including a damping matrix (C), as a linear combination of mass matrix (M) and stiffness matrix (K), as given:

$$C = \alpha M + \beta K \quad (1)$$

where, the coefficients α and β are given by:

$$\begin{Bmatrix}\alpha\\ \beta\end{Bmatrix} = \frac{2D}{\omega_1 + \omega_2}\begin{Bmatrix}\omega_1\omega_2\\ 1\end{Bmatrix} \tag{2}$$

where, D is the damping ratio, and ω_1 and ω_2 are frequencies describing the damping curves in rad/s. The first frequency (ω_1) is defined as the resonant cut-off frequency of layered track substructure. In contrast, the second frequency (ω_2) is calculated as the maximum frequency for a predefined train speed, as given (El Kacimi et al., 2013):

$$f_p = \frac{V_p}{4H} \tag{3}$$

where, H: depth of subgrade; and f_p: the cut-off frequency of the subgrade soils.

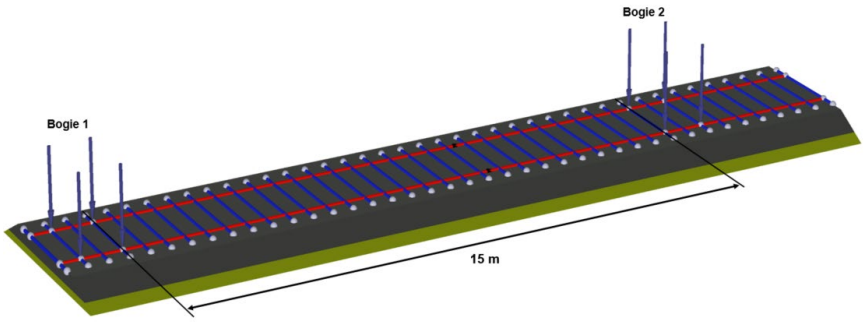

Figure 2. Configuration of two bogie for simulation moving train load, initially placed at sleeper – rail junctions

2.5 **Modelling of Geogrids**

Geogrids were simulated using plate elements built in the PLAXIS 3D, as shown in Figure 3. it is noted that the plate elements have only 5 d.o.f per node as they cannot support torsional moments. These elements are directly integrated over their cross section and numerically integrated using 3 point Gaussian integration. Interface elements were adopted to simulate the interaction between a geogrid and surrounding soils which include pairs of nodes that are numerically integrated using 6-point Gauss integration. Each node can exhibit three translational degrees of freedom (u_x, u_y, u_z); and therefore they can capture differential displacements between elements (i.e., slipping and gapping). The notation of a positive and negative interfaces are presented in Figure 3b showing at which side of the surface the interface

between the adjacent soil and this surface is located. Using interface elements, node pairs are formed at the geogrid-soil interfaces and interacted via two elastic-perfectly plastic springs: one for gap displacement and another for slip displacement.

Initially, a geogrid was placed at the ballast – capping interface as this location was expected to provide the highest degree of reinforcement and therefore, act as a benchmark for comparison (Fig. 3a). Location of geogrids were then varied in the current FEM analysis to be simulated at the: (i) capping – subgrade interface, (ii) middle of ballast layer, and (iii) subballast-subgrade ('SS') interface. Different types of geogrids were also considered by having the axial stiffness (EA) parameters varied from 250 kN/m, 775 kN/m, 1,200 kN/m and 2,000 kN/m to study the effect of grid stiffness on reinforcement. Values for interface strength reduction factor (R_{inter}) were considered to be 0.4, 0.6, 0.8 and 1. At R_{inter} = 1, the interface behaviour is considered rigid. Based on model geometry, material model, input parameters, loading and boundary condition, sensitivity analysis on the modelling of geogrid and effect of geogrid stiffness, the FEM model can be represented.

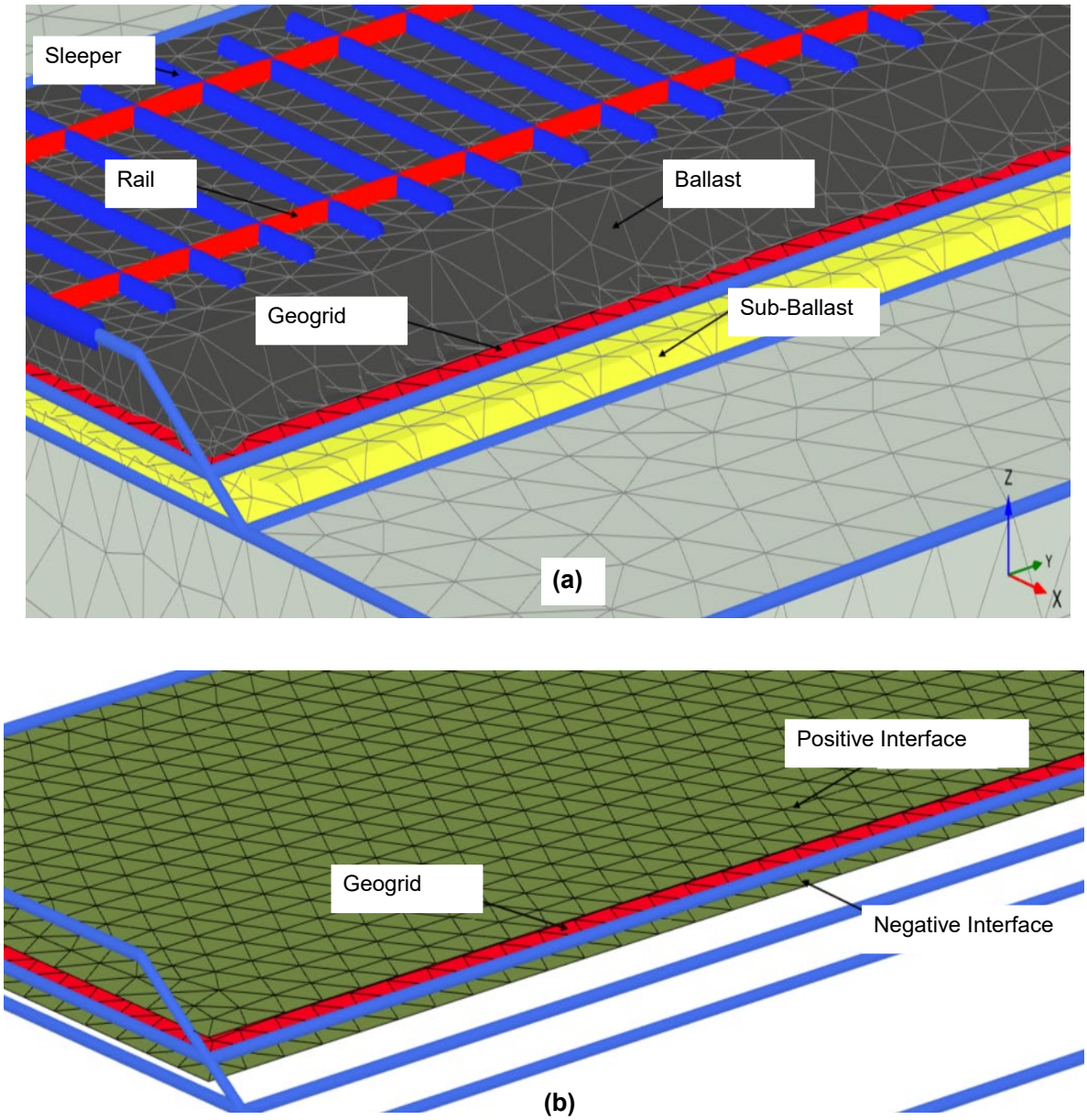

Figure 3. (a) Initial location of geogrid in track, and (b) positive and negative interfaces of geogrid

2.6 **Monitored locations in the track**

Specific nodes and elements at varied locations across the track in the FEM track model were monitored during loading progress. Points of interest were at the sleeper – rail interface (at 2.5, 5, 10, and 15 metres) which are and the midpoint between two sleepers (7.25, 12.25 and 17.75 metres), while along the depths including the track surface, mid-point of ballast layer and ballast shoulder. Measured responses at the ballast shoulder to assess lateral displacement and

directly under the sleeper to measure stress concentrations. Prior to evaluating the effect of geogrid reinforcement, displacements of the unreinforced track were evaluated for the benchmarking purpose. A selected plane is considered at the mid-point of the track, which implies that the rear bogie loading will arrive at approximately 0.5 seconds (Figure 4). On the selected plane, point A was located at centre of track (node A: – 3.75m, 12.25m, 3.15m) where point C and point D were located at the right and the left shoulder, respectively. Vertical cross-sections are examined to assess general deformation characteristics and trends to experience settlement or heaving.

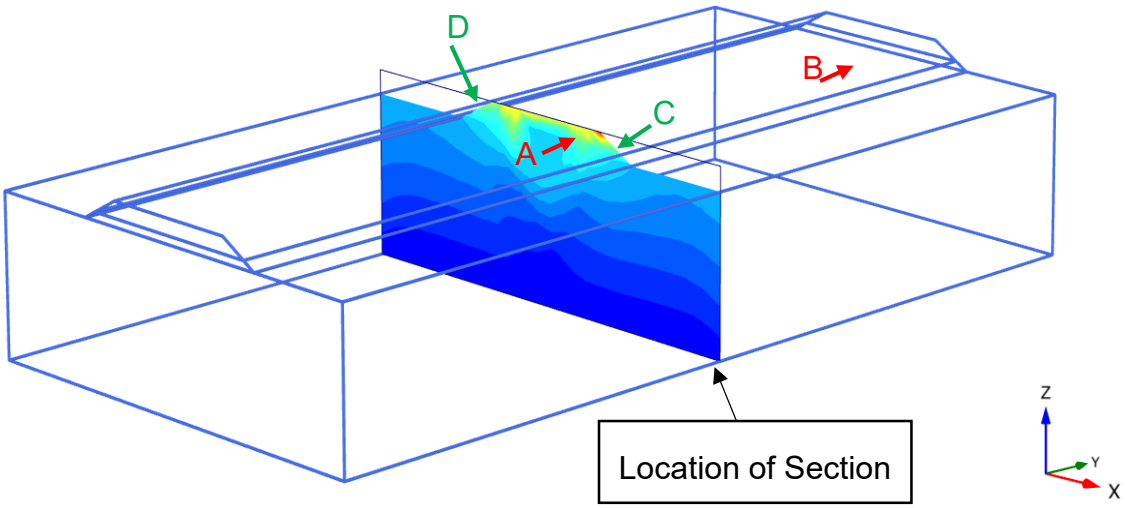

Figure 4. Vertical cross-section to monitor deformation responses of a track

3. Results and Discussion

Results obtained from numerical simulations are analysed in terms of differences in track responses between a traditional (unreinforced) track and geogrid reinforced track. Following this, the parameters that influence the performance of geogrid, including axial stiffness (EA), R_{inter} and placement depth are investigated and discussed in the following sections.

3.1 Predicted Vertical Displacements

Vertical displacements was monitored directly below the sleeper (at x=5, y=variable, z=3.4) across the longitudinal dimension of the track. Figure 5 presents comparisons of predicted vertical settlement (S_v) obtained from the 3D FEM simulations of tracks with and without the

inclusion of a geogrid measured at centre of track (node A: – 3.75m, 12.25m, 3.15m) and near end of track (node B: – 3.75m, 17.75m, 3.15m) while Figure 6 shows settlement contours of tracks with and without the inclusion of geogrid. Results show that at the beginning of loading (around 0.5 second) both reinforced and un-reinforced track exhibit a similar vertical displacement, and this could be due to the fact that the tensile strength of geogrid has not been mobilized. Subsequently, with continued application of moving wheel load, the geogrid-reinforced track shows a lesser settlement compare to the unreinforced track. Following the passage of the train loading, an elastic response is seen with some residual (permanent) deformation. The maximum settlement of unreinforced track was predicted as about 10.38 mm while the reinforced track exhibited as peak settlement of 8.82 mm, indicating about 15% reduction in settlement. This reduction can be explained by the fact that the geogrid acts as a reinforcement layer which increase the bearing capacity of the track substructure, which in turn resulting a decreased vertical settlement. Vertical displacement was also analysed at the near end of track, as shown in Figure 5b. This location similarly proves the tendency of the reinforced track to behave comparably to the unreinforced track in initial phases, but provide better reinforcing effects. It is noted that Figure 5a measures the vertical displacement at the centre of the track captured, and at the time of around 0.6 seconds, there is only one wheel loading at point A, which corresponds to a peak of vertical displacement. In contrast, Figure 5b measures the vertical displacement near the end of the track, and at the time of around 1.0 seconds, there are two wheel loadings on Node B, showing two peaks in displacements. Vertical settlement contours (Figure 6) show that accumulated settlement is highest at nodes directly at or under the sleeper, with a typical range between 14.0 – 16.0 mm. Vertical displacements are concentrated at the ballast – sleeper interface and distribute uniformly across sub-ballast and subgrade. Subgrade soils rebound nearly to original conditions with no residual strains. The ballast and sub-ballast retain permanent deformations of approximately 4 – 6 mm in the vertical directions.

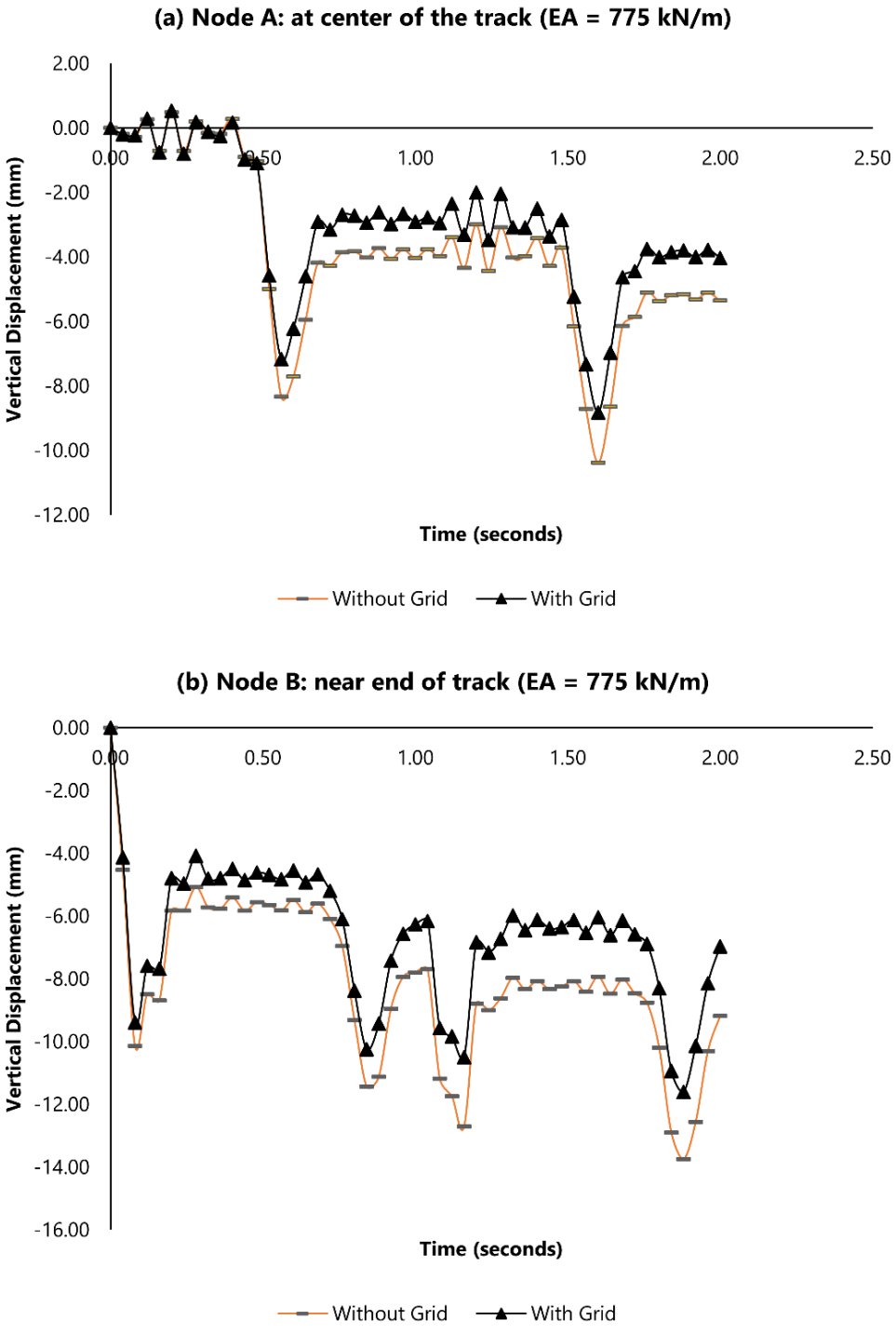

Figure 5. Vertical displacements predicted at: (a) centre of track (node A: – 3.75m, 12.25m, 3.15m); and (b) near end of track (node B: – 3.75m, 17.75m, 3.15m).

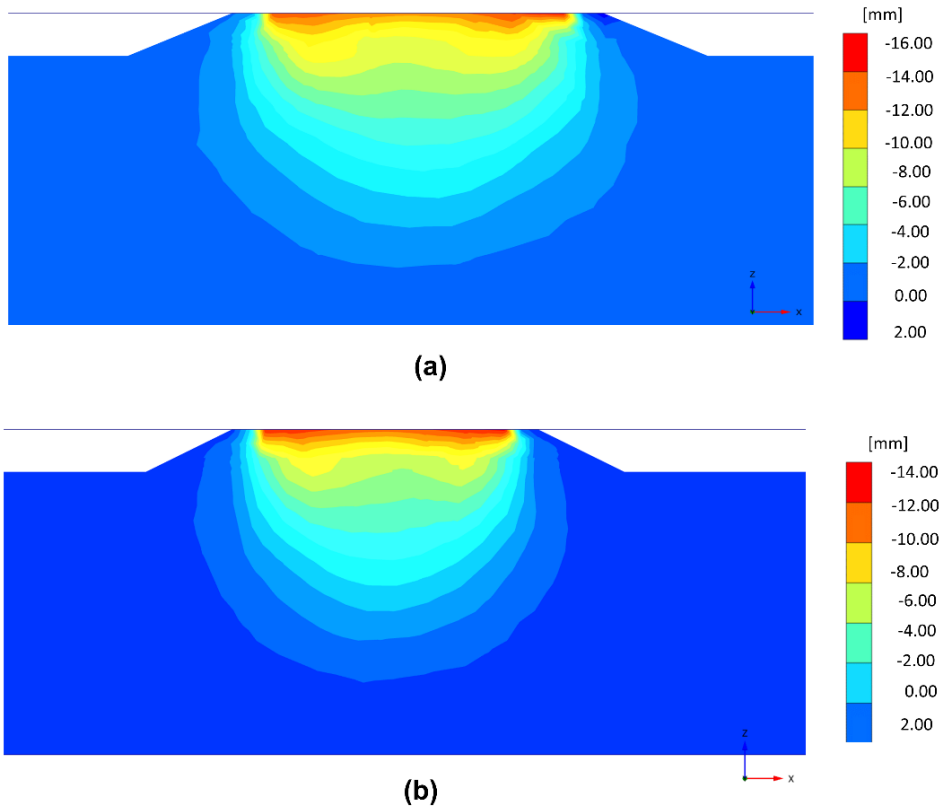

Figure 6. Contours of predicted vertical settlements:(a) without geogrid; and (b) with geogrid

3.2 **Lateral Displacement**

It is noted that the lateral displacement is most pronounced due to the effect of ballast shoulder displaces laterally. Hence, lateral displacement is studied at the shoulders to identify the magnitude of reinforcement provided by geogrid. Flow was studied at nodes in extremities of the shoulder including the right shoulder (node C) and the left shoulder (node D, Figure 4). The left shoulder node is located at the depth of the ballast – capping interface, while the right shoulder node is at the mid-layer of ballast. The predicted lateral displacements obtained from FEM analysis of an unreinforced track in comparison with those predicted for geogrid-reinforced track mesured at the right and left shoulders are presented in Figure 7a and Figure 7b, respectively. Typical lateral displacement contours of tracks with and without the inclusion of geogrid are shown in Figure 8. It is seen that initially a similar lateral displacement is experienced by the both tracks until the unloading (leaving) of the first bogie load. Subsequently, with the arriving of the second loading bogie, a transition zone is present where displacement increases in unreinforced track, but lower in the reinforced track. Compared to unreinforced track, the geogrid-reinforced one exhibits lesser displacement. This effect is likely to continue with increasing load cycles, with a non-linear rate of improvement. In general, the

inclusion of geogrid results in reduced lateral displacements of tracks and this phenomenon is observed for both shoulders. Based on lateral displacement contour (Figure 8), it is seen that the highest retained permanent deformation was at the ballast shoulder with approximately of 3.0 – 4.4 mm of displacement. Hence, the horizontal spreading of ballast and sub-ballast shoulder is the primary mechanism of deformation of tracks.

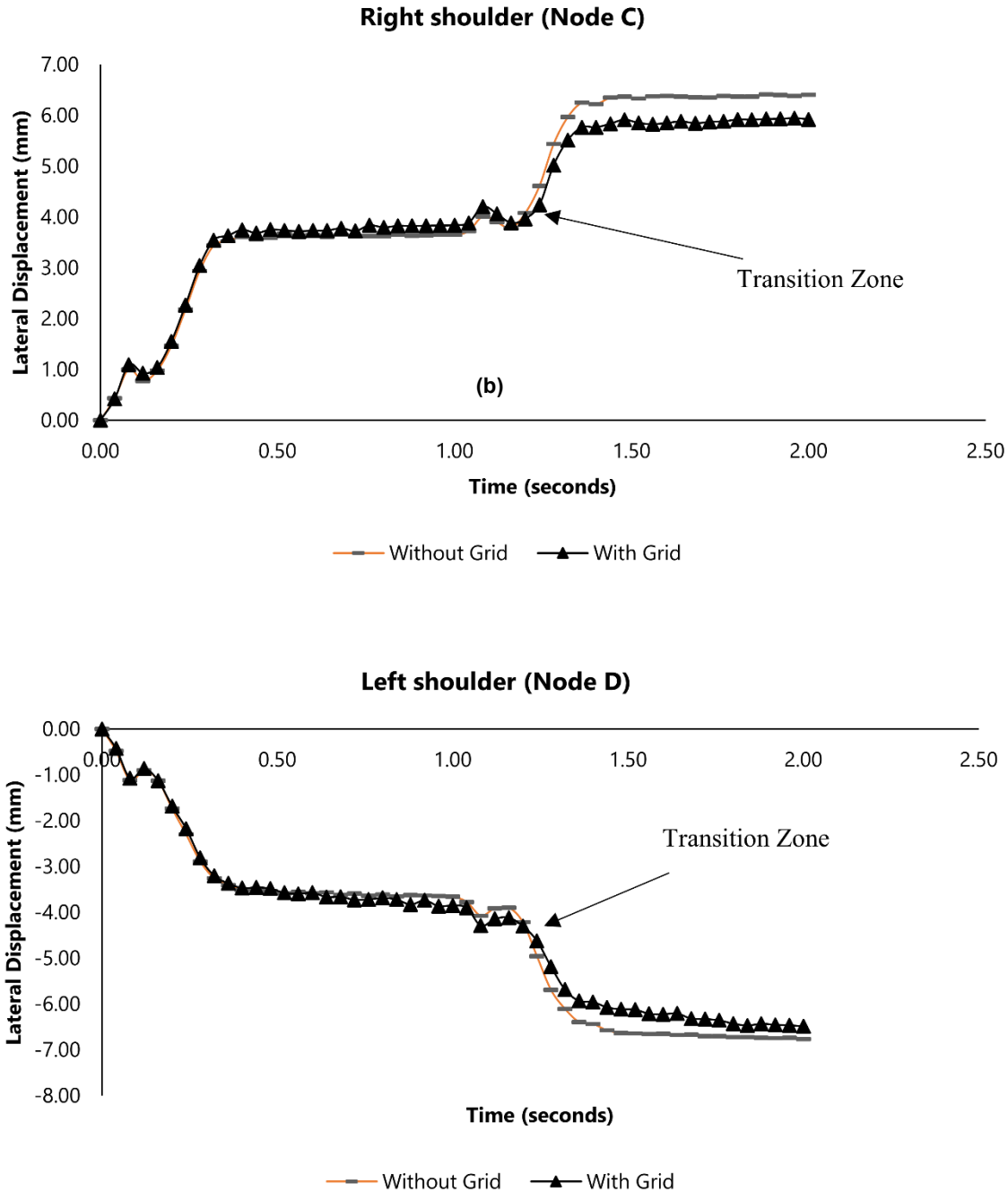

Figure 7. Lateral displacement of ballast at (a) right shoulder (node C); and (b) left shoulder of track (node D)

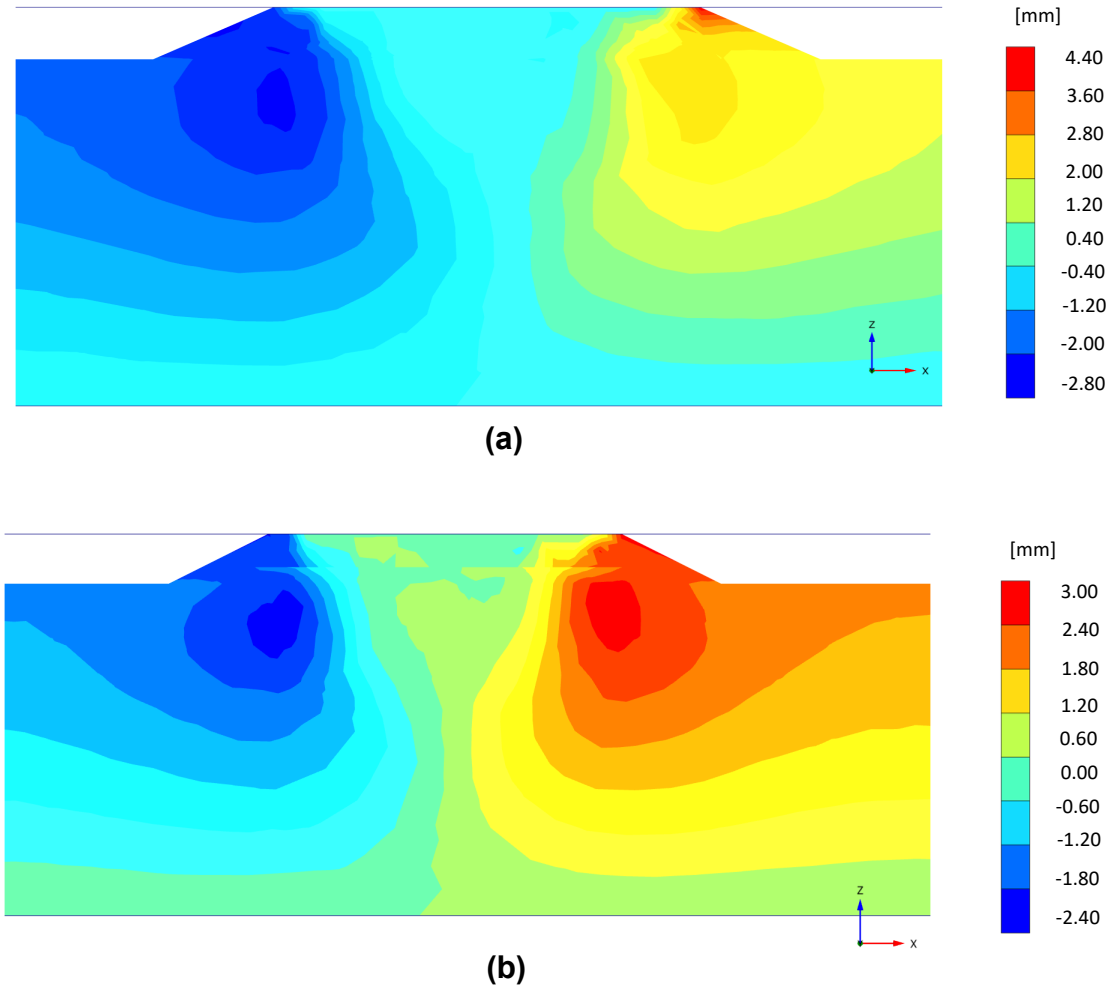

Figure 8. Contours of predicted lateral settlements:(a) without geogrid; and (b) with geogrid

3.3 **Effects of Geogrid Stiffness on Track Deformation**

Geogrids is often assumed to provide limited bending stiffness, and hence, the fundamental parameter governing the behaviour of geogrid is the axial stiffness (EA). To study the effect of geogrid stiffness (EA) on track performance, parametric study was carried out considering the geogrid is as isotropic material having axial stiffness (EA) parameters varied between 250 kN, 775 kN/m, 1,200 kN/m and 2,000 kN/m, as commonly adopted in practice. Typically, an EA of 300 kN is a minimum requirement for rail track application (Yap et al., 2017). Therefore, it would be beneficial to examine the potential reinforcement that is offered by a 250 kN/m grid, and also that provided by significantly stronger stiffness up to EA=2,000 kN/m. Geogrid–ballast interaction and interface behaviour of the material is also influenced by a strength

reduction factor (R_{inter}). A value of R_{inter} =0.8 is adopted here for the purpose of studying the effect of geogrid stiffness on track deformation.

Figure 9a shows the effects of geogrid stiffness on vertical displacements captured at a location below the corner of sleepers. The data reveals that the inclusion of geogrid leads to a decrease in vertical settlements. This observation corroborates the anticipated reinforcement advantages associated with geogrid utilization. The investigation into the effect of different geogrid stiffness values ranging from EA=250-2000 kN/m showed negligible changes in the vertical displacement observed under the sleeper. This lack of significant change can be attributed to the finite element method (FEM) simulations being executed for a scenario involving only 2 bogies (equivalent to 1 train carriage). In this setup, long-term loading, which is necessary to fully activate and demonstrate the influence of geogrid stiffness, was not conducted. As a result, the anticipated effects of varying geogrid stiffness might not have been fully mobilized or demonstrated under these specific simulation conditions. Upon initial loading by a bogie, the findings are interesting as typically all geogrids exhibit very similar in vertical displacement irrespective of varying the geogrid stiffness (EA). However, this is not necessarily surprising as it is understood that geogrids primarily function is to provide lateral confinement to the track through interlocking with surrounding particles and thereby preventing differential track settlements. From this, it is considered likely that the effect of changing EA on vertical displacements will become more pronounced with increased load cycles, as particle rearrangement and densification will be allowed to occur upon the lateral spread of the ballast.

Figure 9b shows the predicted lateral displacement of tracks with geogrid at varying stiffness (EA). Results show that the effect of geogrid reinforcement is more pronounced with increased EA and typically more beneficial with increased passages (i.e., subsequent loading bogies) which further support the hypothesis that the effects of grid interlock require a certain number of loadings prior to fully activating the effect. The displacement indicates the tendency of surrounding particles to move due to the application of moving wheel loads. At a given geogrid stiffness, the reinforced track exhibits a reduced lateral deformation as compared to the unreinforced track, confirming the ability of the geogrid to provide confinement and stabilise the substructure.

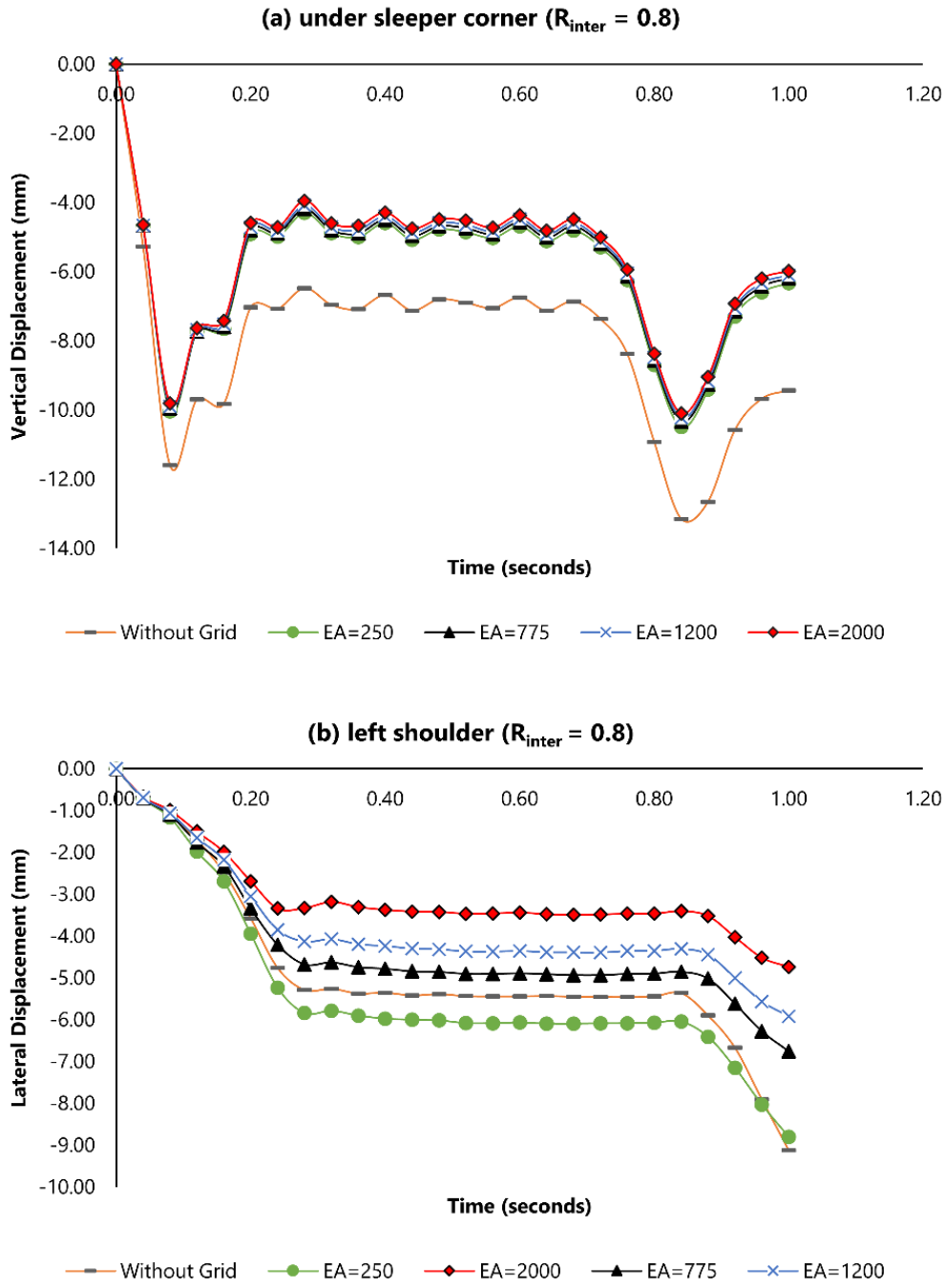

Figure 9: Effect of geogrid stiffness (EA) on track deformation: (a) Vertical settlement; (b) Lateral displacement.

The percentage reduction of lateral displacement associated with the inclusion of geogrid can be seen in Figure 10. As expected, the variations in EA were more pronounced with increased load cycles; and the geogrid with higher stiffness provides higher reduction rate. Interestingly,

the geogrid with highest stiffnees (EA=2,000 kN/m) is able to provide reinforcement from the beginning of loading cycle, exhibiting a relatively high reduction in lateral dispalcement of up to 48.1%. A 775 kN/m grid after a one loading cycle achieved a lateral displacement reduction of 25.9%. However, the geogrid with EA=250 kN/m was seen not to provide any reduction in lateral displacement due to low stiffness which could limited lateral confinement and interlocking. It is noted that the present study assumes strength reduction at the geogrid interfaces, which is likely to occur due to the presence of foreign material, inappropriate particle to grid size, and ballast degradation. The interface strength reduction value (R_{inter}) of 0.8 could be still considered an optimistic estimate if compared to actual conditions of older and less frequently maintained tracks. It is recommended that to truly advance performance of geogrid reinforced track, the interface strength must be optimised and considered in design.

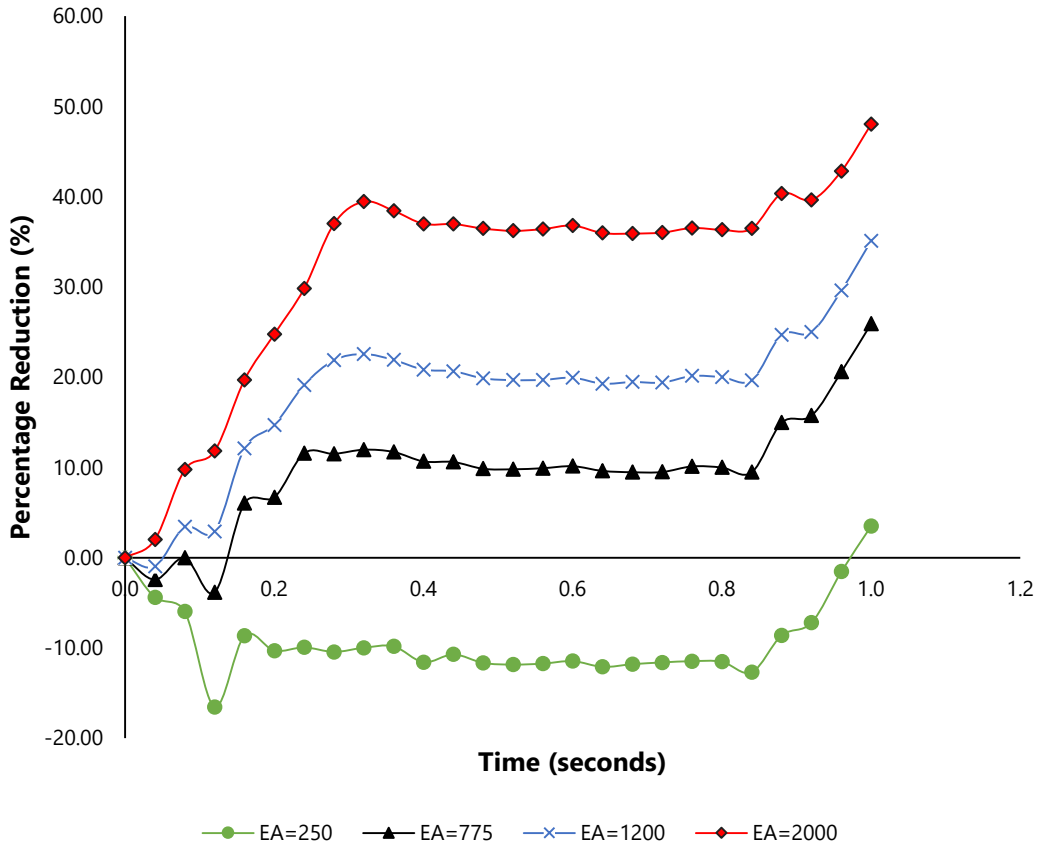

Figure 10. Percentage reduction in lateral displacement due to the inclusion of geogrid

3.4 **Effect of the Interface Properties on Track Deformation**

The influence of interface strength reduction factor (R_{inter}) on the deformation of track was studied by varying the values of R_{inter} from 0.4 to 1.0. A geogrid having EA=775 kN/m was adopted for the current analysis, and predicted results are shown in Figure 11. It is seen that varying R_{inter} has negligible impact on the vertical displacement of the track where the Figure 11a further demonstrates the tendency of all R_{inter} values to experience relatively similar levels of vertical displacement upon a bogie loading. As discussed above, this phenomenon is not likely to continue with increased load cycles, where the differentiation of R_{inter} values to lateral spread of ballast will become more pronounced in subsequent bogie loading.

Lateral displacements in Figure 11b, however, show more typical results where the lowest value of R_{inter} = 0.4 has significantly lower performance as compared to the unreinforced track and all other interface conditions. This is likely because slip conditions have been occurred at the critical location of the ballast – capping interface where shearing forces are high. A value of R_{inter} =0.6 is also seen to offer unnoticeable reduction in lateral displacement as compared to the unreinforced track; however, a marginal reduction occurs from a second loading cycle. The presence of geogrid having R_{inter} values of 0.8 and 1.0 provided more ideal conditions, offering significant reduction in lateral spreading of track, providing ideal confinement under moving train loading.

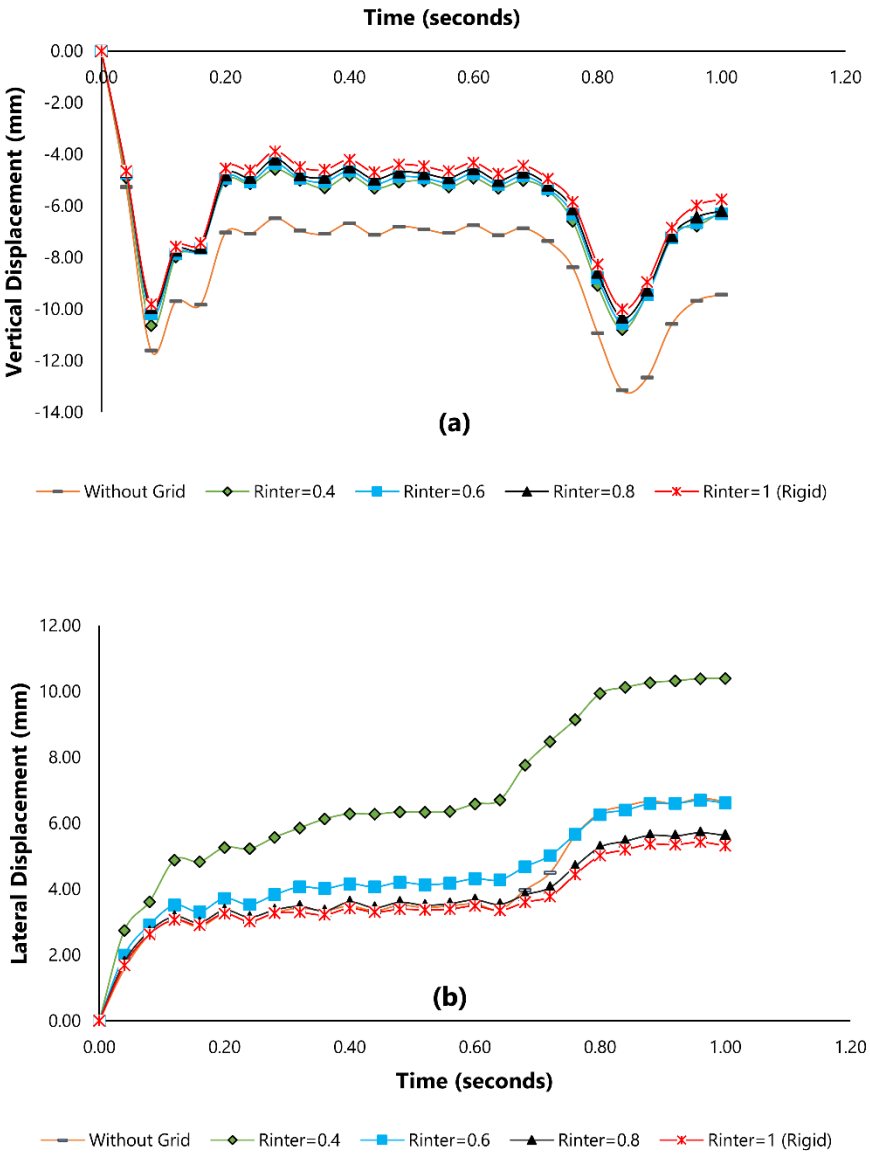

Figure 11. Effect of the interface properties (R_{inter}) on track deformation: (a) Vertical settlement; (b) Lateral displacement

3.5 Effect of Geogrid Placement Location

The impact of placing geogrid at separate locations is investigated at different depths, including at: (i) middle center of the ballast layer, (ii) ballast-subballast ('BS') interface and (iii) subballast-subgrade ('SS') interface. In addition, a two layer of geogrid configuration is also simulated, with one grid at the 'BS' and another grid is at the 'SS' interfaces. A geogrid having EA =775kN/m and R_{inter} =0.8 is used for the current FEM analysis.

Results from Figure 12 show that placing a geogrid at the ballast and sub-ballast interface (location: 'BS') provides the highest reinforcement in terms of reduced track deformation. This indicates that having a geogrid placed underneath the ballast layer provides a greater degree of

reinforcement, as geogrid is likely to laterally confine and interlock with particles. This findings are in agreement with results reported by previous studies (Bathurst and Raymond, 1987; McDowell et al., 2006), among others. In contrast, placing a geogrid at the middle center of the ballast layer does not provide any reinforcement effect and this arrangement should be avoided due to impediment during track maintenance (i.e., ballast tamping). The use of double geogrid configuration provides significant reduction in both vertical and lateral deformation of tracks, as expected. Geogrid provides a reinforcing function to rail track primarily in the form of confinement. Hence, it is unsurprising to see that lateral displacement in a reinforced track is significantly lower than a traditional track.

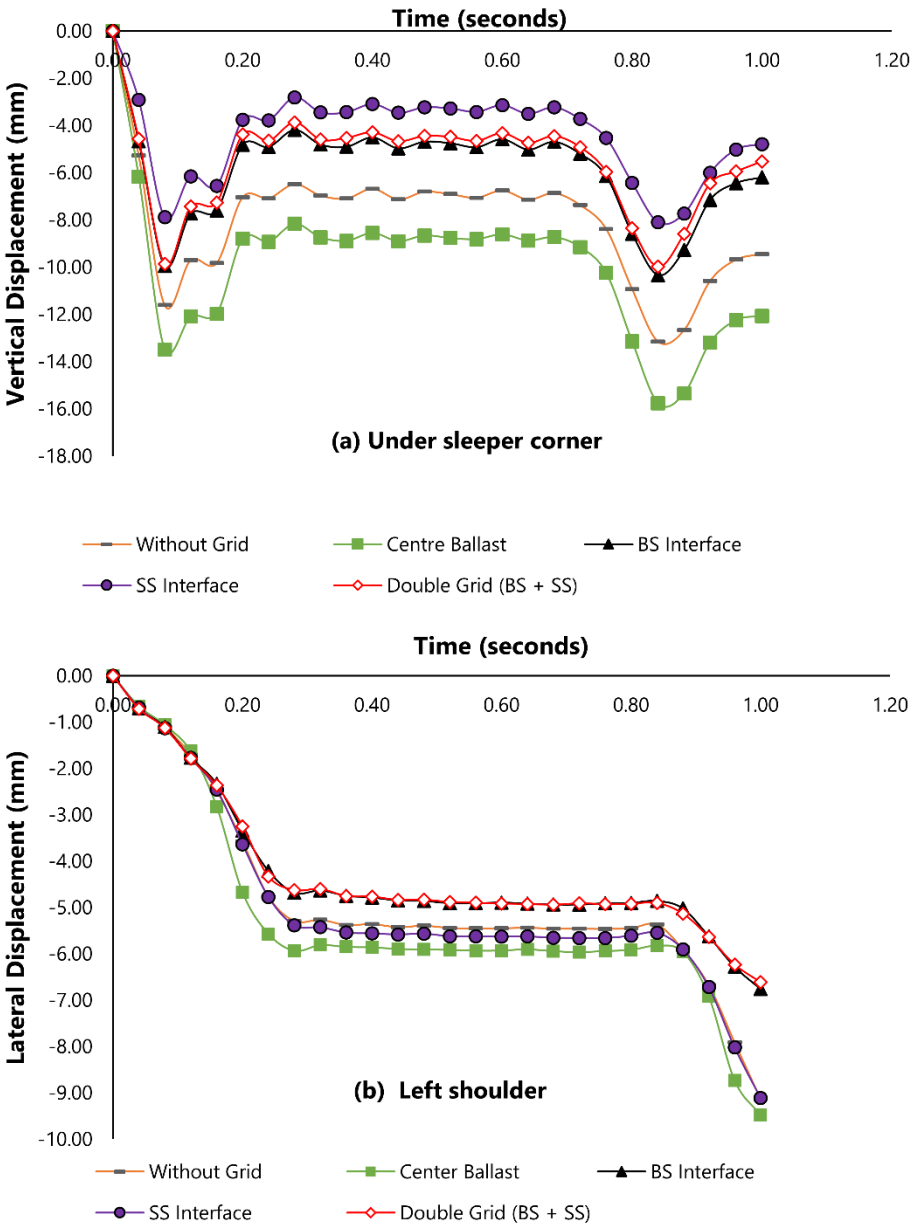

Figure 12. Effect of location of geogrid placement on track deformation: (a) Vertical settlement; (b) Lateral displacement

4. Limitations of the current study

- Model geometry: Due to limited computational resources, the overall model dimensions were restricted to 20 m in the longitudinal direction, which prohibited visualisations of deformation across an adequate length of track. Subgrade soils were up to a depth of 3 m only, with groundwater not considered to be present.
- Loading: The track loading in this study did not consider the effects of impact forces caused by imperfections at the wheel-rail interface, rail abnormalities such as wheel. Furthermore, the moving loads applied is constant with no components of acceleration or braking considered, which is likely to occur in the real tracks.

- The effect of train speeds and different train wheel loading (e..g, passenger versus freight trains) were not considered in the current FEM analysis where there has been only wheel loads of 150 kN traveling as a speed of 72km/h was simulated. Material parameters were selected from previous studies and model calibration and further verification with other studies are recommended.

Nonetheless, the current study is able to numerically capture the effect of different types of geogrid on the deformation responses of ballasted tracks. The study identified a number of key conclusions that influence the performance of tracks, and therein design of geogrid in rail track application. Future work is recommended to overcome the above limitations in development of FEM models, to provide a more accurate capture of the true behaviour of geogrid reinforced rail track.

5. Conclusions

The effects of geogrids have on the deformation responses of ballasted tracks were investigated in this study. Numerical simulations were carried out using three-dimension software package (PLAXIS 3D) on ballasted model tracks with and without the inclusion of geogrids subjected to moving load. Based on numerical results, the main conclusions which could be drawn from this study are listed below:

- Compared to an unreinforced track, the inclusion of geogrid in track exhibited significantly lower magnitudes of vertical and lateral displacement under the application of a moving train load. For instance, with the presence of a geogrid having

EA=775 kN/m, a lateral displacement reduction of 25.9% was achieved, while a geogrid with EA= 2,000 kN/m achieved up to 48.1% lateral reduction.

- The axial stiffness of geogrid is found to impact the vertical and lateral displacements in the track substructure. The weakest grid of EA=250 kN/m was found to produce excessive displacements and therein, is considered unsuitable for adoption in practice. Stronger geogrids having the EA is equal or higher than 775 kN/m demonstrated good results in mitigating displacements and strains accumulated in the substructure.

- The interface property (R_{inter}) posed a significant influence on the deformation of tracks where the lowest value of R_{inter}= 0.4 resulted in the largest displacements. The presence of geogrid having R_{inter} values of 0.8 and 1.0 provided more ideal conditions, offering significant reduction in lateral spreading of track, offering ideal confinement under moving train loading.

- The optimum placement of geogrid as typically agreed by others was found to directly at the ballast and sub-ballast interface. Different locations tested could not provide the same level of reinforcement to the overall ballast layer upon loading. A single geogrid layer was found to be effective in mitigating deformation of ballast.

In summary, the significant findings in this study indicate that the inclusion of a geogrid layer at the ballast and capping interface significantly reduces both vertical and lateral displacement, with greater impact observed under increased loading cycles. Additionally, findings suggest that the axial stiffness of the geogrid affects overall track deformation, while optimal placement is identified directly at the ballast and capping interface

References

Alabbasi, Y., Hussein, M., 2021. Geomechanical modelling of railroad ballast: a review. Archives of Computational Methods in Engineering 28, 815-839.

Basudhar, P.K., Dixit, P.M., Gharpure, A., Deb, K., 2008. Finite element analysis of geotextile-reinforced sand-bed subjected to strip loading. Geotextiles and Geomembranes 26, 91-99.

Bathurst, R.J., Nernheim, A., Walters, D.L., Allen, T.M., Burgess, P., Saunders, D.D., 2009. Influence of reinforcement stiffness and compaction on the performance of four geosynthetic-reinforced soil walls. Geosynthetics International 16, 43–59.

Bathurst, R.J., Raymond, G.P., 1987. Geogrid reinforcement of ballasted track. Transportation Research Record 1153, 8-14.

Brown, S.F., Brodrick, B.V., Thom, N.H., McDowell, G.R., 2007a. The Nottingham railway test facility, UK. Proceedings of the Institution of Civil Engineers - Transport 160, 59-65.

Brown, S.F., Kwan, J., Thom, N.H., 2007b. Identifying the key parameters that influence geogrid reinforcement of railway ballast. Geotextiles and Geomembranes 25, 326-335.

Brown, S.F., Thom, N.H., Kwan, J., 2006. Optimising the geogrid reinforcement of rail track ballast, Railfound Conference, Birmingham, pp. 346-354.

Chen, C., McDowell, G.R., Thom, N.H., 2013. A study of geogrid-reinforced ballast using laboratory pull-out tests and discrete element modelling. Geomechanics and Geoengineering 8, 244-253.

Chua, B.T., Abuel-Naga, H., Nepal, K.P., 2023. Design Charts for Geogrid-Reinforced Granular Working Platform for Heavy Tracked Plants over Clay Subgrade. Transportation Infrastructure Geotechnology 10, 795-815.

Dong, Y.L., Han, J., Bai, X.H., 2010. A numerical study on stress-strain responses of biaxial geogrids under tension at different directions. GeoFlorida 2010: Advances in Analysis, Modeling & Design, ASCE (GSP 199), 2551-2560.

Duncan-Williams, E., Attoh-Okine, N.O., 2008. Effect of geogrid in granular base strength - An experimental investigation. Construction and Building Materials 22, 2180-2184.

El Kacimi, A., Woodward, P.K., Laghrouche, O., Medero, G., 2013. Time domain 3D finite element modelling of train-induced vibration at high speed. Computers & Structures 118, 66-73.

Esveld, C., 2014. Modern railway track. MRT Press, The Netherlands.

Faizan A. A., Kirtel O., Celebi E., Zulfikar A. C., Goktepe F. 2022. Experimental validation of a simplified numerical model to predict train-induced ground vibrations, Computers and Geotechnics 141, 104547

Feng, S.-J., Wang, Y.-Q., 2023. DEM simulation of geogrid–aggregate interface shear behavior: Optimization of the aperture ratio considering the initial interlocking states. Computers and Geotechnics 154, 105182.

Fisher, S., Horvat, F., 2011. Investigations of the reinforcement and stabilasation effect of geogrid layers under railway ballast. Slovak Journal of Civil Engineering 19, 22-30.

Gamal, A.M., Belal, A.M., Elsoud, S.A., 2016. Numerical modeling of geogrid reinforced soil bed under strip footings using finite element analysis, 18th International Conference on Civil and Construction Engineering, Jeddah, Saudi Arabia.

Giannakos, K., 2010. Loads on track, ballast fouling, and life cycle under dynamic loading in railways. Journal of Transportation Engineering, ASCE 136, 1075-1084.

Hadi, M.A., Alzabeebee, S., 2023. Development of a Finite Element Model to Study the Settlement of Ballasted Railway Tracks Subjected to Two Adjacent Moving Trains. Transportation Infrastructure Geotechnology 10, 733-748.

Hussaini, S.K.K., Indraratna, B., Vinod, J.S., 2016. A laboratory investigation to assess the functioning of railway ballast with and without geogrids. Transportation Geotechnics 6, 45-54.

Indraratna, B., Nimbalkar, S., and Rujikiatkamjorn, C. (2012). Track stabilisation with geosynthetics and geodrains, and performance verification through field monitoring and numerical modelling. Int. J. Railway Technol. 1, 195–219. doi: 10.4203/ijrt.1.1.9

Indraratna, B., Rujikiatkamjorn, C., Salim, W., 2023. Advanced Rail Geotechnology - Ballasted Track. CRC Press, Taylor & Francis Group, London, UK.

Jiang, Y., Nimbalkar, S., 2019. Finite element modeling of ballasted rail track capturing effects of geosynthetic inclusions. Frontiers in Built Environment 5, 69.

Konietzky, H., te Kamp, L., Groeger, T., 2004. Use of DEM to model the interlocking effect of geogrids under static and cyclic loading, in: Shimizu, H.c.e. (Ed.), Numerical Modeling in Micromechnics via Particle Methods, pp. 3-11.

Le Pen, L., Watson, G., Hudson, A., Powrie, W., 2018. Behaviour of under sleeper pads at switches and crossings–Field measurements. Proceedings of the Institution of Mechanical Engineers, Part F: Journal of rail and rapid transit 232, 1049-1063.

Li, D., Hyslip, J., Sussmann, T., Chrismer, S., 2015. Railway geotechnics. CRC Press.

Li, F.L., Peng, F.L., Tan, Y., Kongkitkul, W., 2010. Simulating Rate-Dependent Behavior of Geogrid-Reinforced Sands by FEM. GeoFlorida 2010: Advances in Analysis, Modeling & Design (Geotechnical Special Publication, 199), ASCE, 2591-2600.

Luo, Z., Zhao, C., Bian, X., Chen, Y., 2023a. Discrete element analysis of geogrid-stabilized ballasted tracks under high-speed train moving loads. Computers and Geotechnics 159, 105451.

Luo, Z., Zhao, C., Cai, W., Gu, Q., Lin, W., Bian, X., Chen, Y., 2023b. Full-scale model tests on ballasted tracks with/without geogrid stabilisation under high-speed train loads. Géotechnique 0, 1-15.

McDowell, G.R., Harireche, O., Konietzky, H., Brown, S.F., Thom, N.H., 2006. Discrete element modelling of geogrid-reinforced aggregates. Proceedings of the ICE - Geotechnical Engineering 159, 35-48.

Moghadam, M.J., Ashtari, K., 2020. Numerical Analysis of Railways on Soft Soil Under Various Train Speeds. Transportation Infrastructure Geotechnology 7, 103-125.

Nazari, S., Huang, H., Qiu, T., 2022. Identification of railroad ballast fouling through statistical process control on ballast particle movement. Transportation Geotechnics 36, 100780.

Ngo, N.T., Indraratna, B., Rujikiatkamjorn, C., 2016. Modelling geogrid-reinforced railway ballast using the discrete element method. Transportation Geotechnics 8, 86-102.

Perkins, S.W., Edens, M.Q., 2002. Finite Element and Distress Models for Geosynthetic-reinforced Pavements. international Journal of Pavement Engineering 3, 239-250.

Powrie, W., Le Pen, L., Milne, D., Thompson, D., 2019. Train loading effects in railway geotechnical engineering: Ground response, analysis, measurement and interpretation. Transportation Geotechnics 21, 100261.

Sayeed, M.A., Shahin, M.A., 2023. Dynamic Response Analysis of Ballasted Railway Track–Ground System under Train Moving Loads using 3D Finite Element Numerical Modelling. Transportation Infrastructure Geotechnology 10, 639-659.

Selig, E.T., Waters, J.M., 1994. Track geotechnology and substructure management. Thomas Telford, London.

Setiawan, D., 2016. Worldwide Slab Track Development as Consideration for Indonesian Slab Track Design Concept. Konferensi Nasional Teknik Sipil-KoNTekS 10, 441-450.

Shan, Y., Zhou, S., Wang, B., Ho, C.L., 2020. Differential Settlement Prediction of Ballasted Tracks in Bridge-Embankment Transition Zones. Journal of Geotechnical and Geoenvironmental Engineering 146, 04020075.

Tucho, A., Indraratna, B., Ngo, T., 2022. Stress-deformation analysis of rail substructure under moving wheel load. Transportation Geotechnics 36, 100805.

Tutumluer, E., Huang, H., Bian, X., 2012. Geogrid-Aggregate Interlock Mechanism Investigated through Aggregate Imaging-Based Discrete Element Modeling Approach. International Journal of Geomechanics 12, 391-398.

Tutumluer, E., Qian, Y., Hashash, Y.M.A., Ghaboussi, J., Davis, D.D., 2013. Discrete element modelling of ballasted track deformation behaviour. International Journal of Rail Transportation 1, 57-73.

Varandas, J.N., Paixão, A., Fortunato, E., Zuada Coelho, B., Hölscher, P., 2020. Long-term deformation of railway tracks considering train-track interaction and non-linear resilient behaviour of aggregates – a 3D FEM implementation. Computers and Geotechnics 126, 103712.

Yap, H.C., Khabbaz, H., Singh, J., 2017. Numerical analysis of geosynthetics and engineering fill in performance of reconditioned ballasted track. Australian Geomechanics Journal.